Thermal effect on magnetoexciton energy spectra in monolayer transition metal dichalcogenides

Duy-Nhat Ly,[1,*,†] Dai-Nam Le,[2,*,‡] Ngoc-Hung Phan,[1] and Van-Hoang Le[1,§]

[1]*Computational Physics Key Laboratory K002, Department of Physics, Ho Chi Minh City University of Education, Ho Chi Minh City 72759, Vietnam*

[2]*Department of Physics, University of South Florida, Tampa, Florida 33620, USA*

(Received 27 September 2022; revised 2 March 2023; accepted 29 March 2023; published 7 April 2023)

It is widely comprehended that temperature may cause phonon-exciton scattering, enhancing the energy level's linewidth and leading to some spectrum shifts. However, in the present paper, we suggest a different mechanism that allows the thermal motion of the exciton's center of mass (c.m.) to affect the magnetoexciton energies in monolayer dichalcogenides (TMDCs). By the nontrivial but precise separation of the c.m. motion from an exciton in a monolayer TMDC with a magnetic field, we obtain an equation for the relative motion containing a motional Stark term proportional to the c.m. pseudomomentum, related to the temperature of the exciton gas but neglected in the previous studies. Solving the Schrödinger equation without omitting the motional Stark potential at room temperature shows approximately a few meV thermal-magnetic shifts in the exciton energies, significant enough for experimental detection. Moreover, this thermal effect causes a change in exciton radius and diamagnetic coefficient and enhances the exciton lifetime as a consequence. Surprisingly, the thermoinduced motional Stark potential breaks the system's SO(2) symmetry, conducting new peaks in the exciton absorption spectra at room temperature besides those of the *s* states. This mechanism could be extended for other magnetoquasiparticles such as trions and biexcitons.

DOI: 10.1103/PhysRevB.107.155410

I. INTRODUCTION

During the last two decades, monolayer transition-metal dichalcogenides (TMDCs) have become hot spots for studying the formation of excitons because of their unique property of electron-hole interaction [1–4]. Unlike three-dimensional excitons in novel semiconductors, neutral excitons in these monolayer TMDCs are thermally stable at room temperature, even for the Rydberg states. Their high binding energy provides beneficial optical properties in both ultraviolet (UV) and infrared (IR) ranges [5–9]. Especially, exciton energy spectra under the presence of a constant magnetic field have been of great interest recently both in experimental observations and theoretical studies due to their incredible potential in retrieving several physical quantities of monolayer TMDCs, such as effective masses of electrons and holes, the Landé *g* factors, and two-dimensional polarizability [10–22]. Therefore, it is essential to qualitatively (and quantitatively, if possible) comprehend the influences of external factors like temperature on the energy spectra of magnetoexcitons in the monolayer TMDCs.

The thermal effect on the exciton energies has been intensively investigated recently and explained by the exciton-phonon scattering [23,24]. Indeed, the quantization of the crystal lattice oscillation results in quasiparticles named *phonons* which carry the thermal motion. The scattering between excitons and phonons affects the relative motion of the electron-hole pair that, consequently, causes some energy shifts of the exciton bound states. Recently, experiments for exciton energies in monolayer TMDCs have been conducted with a high magnetic field [19–21], raising another question related to the center of mass (c.m.) separation. It is well known that the c.m. of a two-body system in a magnetic field can be separated, but the c.m. pseudomomentum remains in the equation for relative motion [25–27]. This circumstance leads to a mechanism that the thermal motion of the c.m. can affect the exciton energies. We will show in the present paper additional energy shifts caused by this thermal-magnetic effect.

The exciton-phonon scattering at finite temperatures affects the imaginary part of exciton energy that makes exciton decay [3,28–34]. However, in our thermal-magnetic mechanism, the motional Stark potential, linearly proportional to the magnetic intensity, could be more inconspicuous than the diamagnetic potential depending on the squared magnetic intensity and may contribute only to the energy shift but not to the exciton lifetime. Nevertheless, this thermoinduced potential could make the average radius of the electron-hole pair larger and consequently enhance the radiative lifetime of excitons in monolayer TMDCs [29,33,34]. Besides, the symmetry breaking of the system due to the additional thermoinduced term can affect the wave functions. Therefore, we aim to examine the effect of finite temperature on the exciton energy spectra, the diamagnetic coefficient, and the exciton radius as a function of magnetic intensity and their consequence on the absorption spectra and the exciton radiative lifetime.

The rest of this paper is as follows. Section II presents the theoretical background for our paper, including the separation of the c.m. motion, the introduction of the motional

*These authors contributed equally to this work.
†nhatld@hcmue.edu.vn
‡dainamle@usf.edu
§hoanglv@hcmue.edu.vn

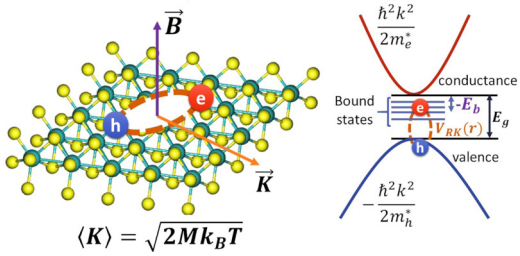

FIG. 1. Excitons in a monolayer TMDC with a magnetic field. The c.m. pseudomomentum is conserved and related to the thermal motion.

Stark potential, and the assumption about its temperature dependence. Then, the results and discussion are given in Sec. III with the thermal effect on the diamagnetic coefficients, the thermal-magnetic shift on exciton energies, the thermoinduced symmetry breaking and enhancement of exciton lifetime, and the new peaks in absorption spectra. Section IV includes our conclusion.

II. THEORETICAL BACKGROUND

A. Schrödinger equation

To consider the thermal effect, we need to solve the Schrödinger equation of the electron-hole pair in the framework of the effective mass approximation, where a Wannier exciton in a monolayer TMDC is described as a two-dimensional system of one electron and one hole interacting with each other by the potential $\hat{V}_{h\text{-}e}(r)$ in the xy plane, as shown in Fig. 1. Because of the two-dimensional many-particle effect, the interaction potential $\hat{V}_{h\text{-}e}$ is no longer Coulombic but screened and described by the Rytova-Keldysh potential [1,2,35–38]. One required task before solving the Schrödinger equation is to separate the movement of the electron-hole c.m with the coordinate $\mathbf{R}$. However, for a two-body system such as an exciton in a magnetic field $\mathbf{B} = B\mathbf{e}_z$, the c.m. dynamics cannot be removed totally from the equation describing the electron-hole relative motion. The variable-separation procedure for this system is no longer trivial because the magnetic field breaks the system's translation symmetry, which leads to the nonconservation of the total momentum $\mathbf{P}$ of the electron-hole pair. Fortunately, there is instead another constant of motion, pseudomomentum $\hat{\mathbf{P}}_0 = \hat{\mathbf{P}} - \frac{1}{2}e\mathbf{B}\times\mathbf{r}$, commuting with the system's Hamiltonian, i.e., $[\hat{\mathbf{P}}_0, \hat{H}_X] = 0$. Using this conservative quantity, one can obtain an equation for the relative motion [25–27]. In this case, the wave function can be written as

$$\Psi_{\mathbf{K}}(\mathbf{R},\mathbf{r}) = e^{\frac{i}{\hbar}(\mathbf{K}+\frac{1}{2}e\mathbf{B}\times\mathbf{r})\cdot\mathbf{r}}\,\psi_{\mathbf{K}}(\mathbf{r}), \tag{1}$$

where $\mathbf{K}$ is an eigenvector of operator $\hat{\mathbf{P}}_0$. The wave function for relative motion $\psi_{\mathbf{K}}(\mathbf{r})$ is obtained by solving the Schrödinger equation

$$\left\{\frac{\hat{\mathbf{p}}^2}{2\mu} + \frac{1-\sigma}{1+\sigma}\frac{eB}{2\mu}\hat{l}_z + \frac{e^2B^2}{8\mu}r^2 + \hat{V}_{h\text{-}e}(r) - \frac{e}{M}(\mathbf{B}\times\mathbf{K})\cdot\mathbf{r} - E\right\}\psi_{\mathbf{K}}(\mathbf{r}) = 0 \tag{2}$$

with the total mass $M = m_e^* + m_h^*$, the exciton reduced mass $\mu = m_e^*m_h^*/(m_e^* + m_h^*)$, and the ratio of masses $\sigma = m_e^*/m_h^*$. Here, m_e^* and m_h^* are the effective masses of the electron and hole; e is the elementary charge with the positive value; $\hat{\mathbf{p}}$ and $\hat{l}_z$ are the operators of the momentum and angular momentum of the relative motion. A detailed derivation of Eq. (2) is given in Supplemental Material [39].

For the exciton in monolayer TMDCs such as WSe_2 as considered in this paper, the exciton reduced mass $\mu = 0.20\times m_e$, mass ratio $\sigma = 0.94$, total mass $M = 0.80\times m_e$ (m_e is electron mass), and the Rytova-Keldysh potential's parameters (the average dielectric constant of the surrounding material $\kappa = 4.5$, screening length $r_0 = 4.21$) are taken from Refs. [15,20].

B. Thermoinduced motional Stark potential

In Eq. (2), we consider the specific term $V_{mS} = -\frac{e}{M}(\mathbf{B}\times\mathbf{K})\cdot\mathbf{r}$ containing the c.m. pseudomomentum $\mathbf{K}$ and will show its relation to the temperature of the neutral exciton gas. First, we note that the density of excitons n_X in monolayer TMDCs is low, i.e., the average distance between two excitons $1/\sqrt{n_X}$ is much larger than the thermal wavelength $\lambda_{th} = \sqrt{\frac{2\pi\hbar^2}{Mk_BT}}$ so that the Maxwell-Boltzmann statistics is still valid. Indeed, the density n_X, i.e., the number of neutral excitons per unit of area, could be modulated around 10^{11}–10^{12} cm^{-2} in real experiments for monolayer WSe_2 [40–43], which is much smaller than its limit at room temperature $\lambda_{th}^{-2} = 4.3\times10^{12}$ cm^{-2}. Then, we estimate the root-mean square of the c.m. pseudomomentum at temperature T by the equipartition theorem as $\frac{1}{2M}\overline{K^2} = k_BT$, where k_B is the Boltzmann constant. Instead of calculating exciton energies at each pseudomomentum value and then averaging them as $\overline{E(K)}$, we do it another way by calculating the exciton energy $E(\overline{K})$ at the average pseudomomentum value. The validity of this approach has been confirmed numerically in Table S-I in Supplemental Material [39]. This approach allows the considered potential to relate to the temperature as follows:

$$V_{mS}(\mathbf{r}) = -\sqrt{\frac{2k_BT}{M}}eB\,x. \tag{3}$$

Here, without losing generality, we consider the case where $\mathbf{K}$ is along the y axis so that vector $\mathbf{B}\times\mathbf{K}$ is along the x axis. A more microscopic grounding for the thermoinduced term (3) is given in Secs. S-I and S-II in Supplemental Material [39].

The potential (3) influences the exciton in the same way as the Stark effect [44,45], so we call it the *thermoinduced motional Stark potential*. Recent theoretical studies of magnetoexcitons in monolayer TMDCs always neglect this potential [14,18,21] that is reasonable only at zero temperature. However, the experimental observations were conducted not only at low temperatures [11,13,15–17,19,20] but also at room temperature [9,10,23,24]. Hence, the motional Stark effect arising from the thermal fluctuation of the c.m. pseudomomentum needs to be considered when calculating the energy spectra of magnetoexcitons in monolayer TMDCs.

We can see that the diamagnetic term $V_{\text{diamag.}}(\mathbf{r}) = \frac{e^2B^2}{8\mu}r^2$ in the effective potential of Eq. (2) is quadratically proportional to the electron-hole distance and consequently dominant at the large separation of the electro-hole pair

TABLE I. Zero-field energies, squared radius, and polarizability.

	$1s$	$2s$	$3s$	$2p_{-1}$	$2p_{+1}$
$E^{(0)}_{nm}$ (eV)	−0.1686	−0.0386	−0.0166	−0.0498	−0.0498
$\langle r^2\rangle_{nm}$ (nm^2)	2.63	45.8	241	21.1	21.1
α_{nm} (nm^2/eV)	3.91	−112	−6060	259	240

compared to the thermoinduced Stark term, which is linearly proportional to the variable x. As a result, there is no tunneling effect, even considering the thermoinduced motional Stark potential. The exciton is always in its bound states, unlike the well-known LoSurdo-Stark effect in the two-dimensional electron gas [46,47] and field-induced dissociation of excitons in a TMDC [48]. Instead of tunneling, we expect the thermoinduced motional Stark potential could cause the Stark shift in the energy spectra.

III. RESULTS AND DISCUSSION

A. Thermal effect on diamagnetic coefficient and Landau levels

To see how the thermoinduced motional Stark potential affects the asymptotic behaviors of exciton energies in the limits of low and high magnetic intensities, we calculate the energies analytically by applying the perturbation theory to the Schrödinger equation (2). For low magnetic intensity, restricted by the condition that the typical length in the magnetic field is much larger than the average exciton radius, $l_B = \sqrt{\hbar/eB} \gg \langle r\rangle_{nm}$, we have the energy of the (n, m) quantum state in the second perturbation order as

$$E^{(2)}_{nm}(B,T) = E^{(0)}_{nm} + \frac{1-\sigma}{1+\sigma}\frac{m\hbar}{2\mu}eB + \frac{\langle r^2\rangle_{nm}}{8\mu}e^2B^2 - \alpha_{nm}\frac{k_BT}{M}e^2B^2, \quad (4)$$

where $E^{(0)}_{nm}$, $\langle r^2\rangle_{nm}$, and α_{nm} are the zero-field energy, squared radius, and polarizability of the exciton. To calculate these quantities, we need to solve the Schrödinger equation in the zeroth order of approximation. However, the solutions cannot be obtained analytically, so, we do it another way by numerically solving Eq. (2) and then fitting the obtained results to formula (4). The concrete values are presented in Table I for $1s$, $2s$, $3s$, $2p_{-1}$, and $2p_{+1}$ states.

The last term in the exciton energy (4), the motional Stark correction, is quadratically proportional to the magnetic field (see also Fig. S-2 in Supplemental Material [39]). That means the thermal effect contributes to the diamagnetic coefficient σ_{nm} defined by the equation

$$\sigma_{nm}(T) = \lim_{B\to 0}\frac{1}{2}\frac{\partial^2 E_{nm}(B,T)}{\partial B^2} = \frac{e^2}{8\mu}\langle r^2\rangle_{nm} - \frac{e^2}{M}\alpha_{nm}k_BT. \quad (5)$$

Table II shows some values for the zero-temperature diamagnetic coefficient $\sigma^0_{nm} = \frac{e^2}{8\mu}\langle r^2\rangle_{nm}$ and their thermoinduced corrections $\Delta\sigma_{nm} = -\frac{e^2}{M}\alpha_{nm}k_BT$ for the $1s$, $2s$, $3s$, $2p_{-1}$, and $2p_{+1}$ states at room temperature. The thermoinduced corrections are about 8% for $1s$, 13% for $2s$, and extremely high for higher states: $2p_{+1}$, $2p_{-1}$, and $3s$ (56, 60, and 130%). These are significant enough to impact experimental measurement that we should pay attention to them when measuring exciton energies at finite temperatures.

TABLE II. Zero-temperature diamagnetic coefficients and their thermoinduced corrections at room temperature in units of μeV/T^2 compared to the experimental data [15].

	$1s$	$2s$	$3s$	$2p_{-1}$	$2p_{+1}$
σ_{nm}[15]	0.31 ± 0.02	4.6 ± 0.2	22 ± 2		
σ^0_{nm}	0.289	5.039	26.53	2.429	2.429
$\Delta\sigma_{nm}$	−0.022	0.637	34.42	−1.469	−1.361
$\frac{\lvert\Delta\sigma_{nm}\rvert}{\sigma^0_{nm}}$	8%	13%	130%	60%	56%

For high magnetic intensity, restricted by condition $l_B = \sqrt{\hbar/eB} \ll \langle r\rangle_{nm}$, the harmonic oscillator potential becomes dominant compared to the Rytova-Keldysk potential. In this case, the main part of the Hamiltonian is the magnetic term; therefore, we can obtain the Landau levels for energies with the thermoinduced Stark corrections by the perturbation theory as

$$E^{(2)}_{nm}(B,T) = \frac{\hbar}{2\mu}\left(2n - |m| - 1 + \frac{1-\sigma}{1+\sigma}m\right)eB - \frac{8\mu\beta_{nm}}{M}k_BT, \quad (6)$$

where the dimensionless coefficients β_{nm} are independent of the temperature T (see details in Supplemental Material [39]). Because of the neglect of Coulomb interaction, the energy formula (6) is valid only for very high magnetic intensity, extremely higher than the laboratory limit of about 91 T [20]. Nevertheless, this formula gives the right rule for thermoinduced shifts from the Landau levels $\Delta E = -\frac{8\mu\beta_{nm}}{M}k_BT$, i.e., linearly proportional to the temperature and almost independent of the magnetic field (see also Fig. S-3 in Supplemental Material [39]).

B. Thermal-magnetic shift on exciton energies

We now numerically investigate the thermal effect on energy by the Feranchuk-Komarov operator method [18,49]. The obtained energies are given in Tables S-II–S-VI in Supplemental Material [39] for the $1s$, $2s$, $3s$, $2p_{-1}$, and $2p_{+1}$ states. For an illustration of the effect, Figs. 2(a) and 2(b) show exciton energies depending on the magnetic intensity at 0 and 300 K.

We see that the temperature does not influence the $1s$ state much. At the same time, the thermal effect is noticeable for the $2s$ and higher Rydberg states for the magnetic intensity of more than 60 T. Particularly for the magnetic intensity of 90 T, the energy shifts when including the temperature of 300 K are shown in Table III. These shifts are big enough compared to the experimental sensitivity of 1 meV and are caused by the thermal motion of excitons in a magnetic field; thus, we call them the *thermal-magnetic shifts*.

We note that the thermal-magnetic shift predicted above is comparable with the shift caused by the phonon-exciton

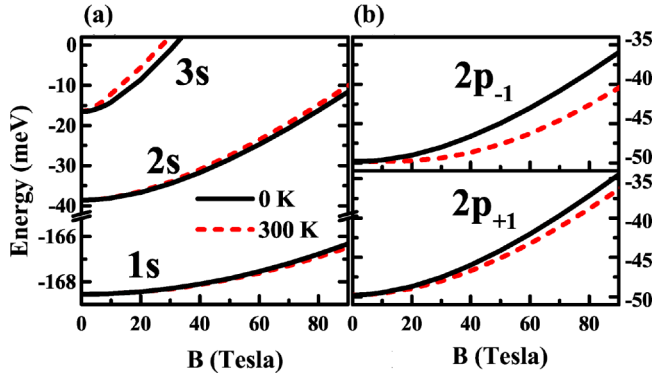

FIG. 2. Exciton energies for the (a) $1s$, $2s$, and $3s$ and (b) $2p_{-1}$ and $2p_{+1}$ states depending on the magnetic intensity B at temperatures 0 and 300 K.

interaction [23,24]. For example, the polaron shift is about 15 meV at room temperature for the $1s$-state exciton in the monolayer TMDC as shown in Ref. [24]. Compared with this, the thermal-magnetic shift for the $1s$ state, which is 0.2 meV as shown in Table III, can be ignored. It means that neglecting the exciton c.m. motion in Ref. [24] is feasible in this case. However, for a higher excited state such as $3s$, the thermal-magnetic shift of 3.9 meV should be taken into account if the polaron shift is calculated within the presence of a high magnetic field. The two shifts are from different mechanisms (phonon-exciton scattering versus the thermal motion of the exciton c.m. in a high magnetic field). They can be calculated separately, and both deserve consideration in analyzing experimental data for excited states in a high magnetic field. Also, for a high magnetic field of about 30 T, as considered in Ref. [50], the fine structure energy split of excitons in monolayer TMDCs caused by the spin-magnetic interaction is up to tens of meV. Compared with this, the thermoinduced shift in the present paper is relatively noticeable, and it is important to consider.

C. Thermoinduced symmetry breaking and enhancement of exciton lifetime

It is well known that the system of a two-dimensional exciton in a magnetic field, perpendicular to the monolayer TMDC plane, has the potential energy dependent on radius $r = \sqrt{x^2 + y^2}$ only and consequently possesses the SO(2) symmetry. However, if included, the thermoreduced motional Stark potential (3), which depends on the angle φ as $\sim r\cos\varphi$, will break this symmetry. In this case, the angular momentum l_z is not conserved, and the magnetic number m is no longer a good quantum number. The consequence is that there are no true s states anymore, but only mixed states with $m \neq 0$ from

TABLE III. Thermal-magnetic shifts in exciton energy spectra calculated between the temperatures of 0 and 300 K for the magnetic field of 90 T.

	$1s$	$2s$	$3s$	$2p_{-1}$	$2p_{+1}$
ΔE (meV)	0.2	1.5	3.9	4.5	1.9

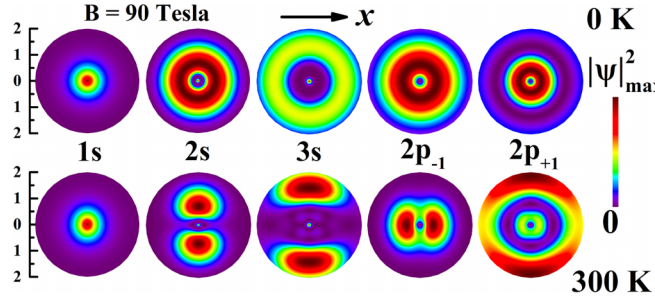

FIG. 3. Deformation of wave functions due to the thermoinduced symmetry breaking.

the basis set functions; see Fig. 3 for the thermoinduced deformation of wave functions. More about the symmetry-breaking effect on the wave function deformation can be found in Sec. S-IV C in Supplemental Material [39].

The wave function deformation leads to the change of the exciton radius, essential for the exciton radiative lifetime $\tau_{\rm rad}$, which is related to the average electron-hole distance $\langle r\rangle$ by the scaling law $\tau_{\rm rad} \sim \langle r\rangle^{\xi}$ [28,34]. The scaling factor ξ mainly depends on the dimensionality of the exciton. We roughly take the value of $\xi \approx 3.5$ extracted by studying the exciton in hBN, diamond, and silicon provided in Ref. [34].

To have an analytical estimation, we get the formula for the exciton radius of s states by the perturbation theory in the low magnetic field limit as

$$\langle r\rangle_T = \langle r\rangle + g\,e^2B^2\frac{k_BT}{M}, \tag{7}$$

where the radius $\langle r\rangle_T$ is calculated using the wave functions with thermal effect. In contrast, the free-field wave functions are used to calculate $\langle r\rangle$. The coefficient g has the following values: 0.17×10^{-3}, 0.04, and -7.5 nm^3/meV^2 for $1s$, $2s$, and $3s$ states, respectively. Consequently, we can get the following formula:

$$\frac{\Delta\tau_{\rm rad}}{\tau_{\rm rad}} = \xi\,\frac{\Delta\langle r\rangle}{\langle r\rangle} \tag{8}$$

for the thermal correction $\Delta\tau_{\rm rad}$ to the exciton radiative lifetime, where $\Delta\langle r\rangle = ge^2B^2\frac{k_BT}{M}$ for the low magnetic intensity. The correction $\Delta\langle r\rangle$ should be calculated numerically for the high magnetic field. We estimate the ratio (8) for the $1s$, $2s$, and $3s$ states at room temperature and magnetic field of 90 T and get the following values: 1.4, 4.9, and 2.1%, relatively considerable. The thermoinduced correction to the radiative lifetime (8) qualitatively agrees with the first-principle calculations and experimental observations given in Refs. [30,31,33] for the $1s$ state, meaning that it always enhances the lifetime and is linearly proportional to the temperature. The thermal motion also causes the lifetime to be enhanced for the $2s$ state but reduced for the $3s$ state. Therefore, this effect (enhancement/reduction of the lifetime) needs further investigation for higher states in our next work.

D. New peaks in absorption spectra due to the symmetry breaking

Interestingly, the system's symmetry breaking at room temperature can lead to new peaks in the magnetoexciton

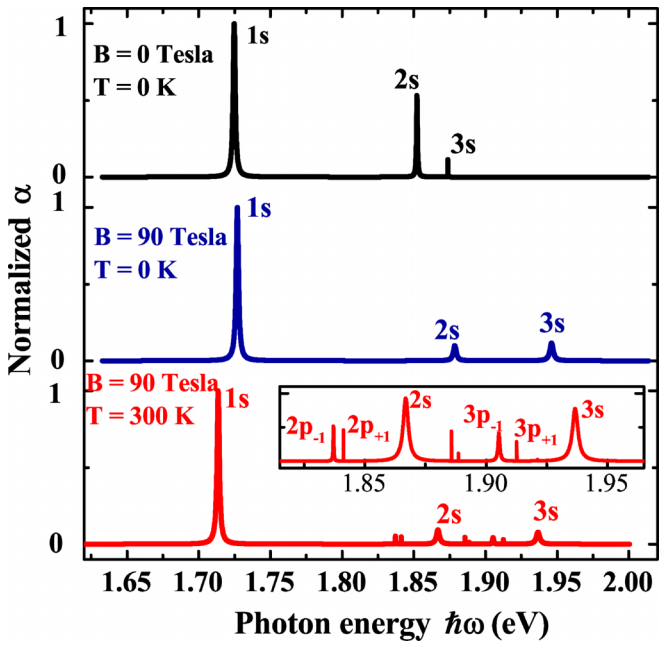

FIG. 4. Normalized optical absorption spectra at temperature 0 K (black and dark blue) and at room temperature (red).

absorption spectra, as shown in Fig. 4. First, we calculate the imaginary part of the susceptibility by the Elliot formula as

$$\alpha(\omega) = C\,\mathrm{Im}\sum_{n,m}\frac{\omega\,|\psi_{nm}(\mathbf{r}=0)|^2}{E_{nm}+E_g-\hbar\omega+i\hbar\tau^{-1}} \tag{9}$$

based on the linear response theory of the exciton [51–54]. We use this quantity to estimate the absorption spectra since they are proportional. Here, the coefficient C depends on the materials' background refractive index and interband transition dipole matrix elements. We are only interested in the general picture and thus choose C to normalize the free-field $1s$ state peak to 1 and then use it as a constant for all other states.

In Eq. (9), the band-gap energy is taken by $E_g = 1890$ meV from the experiment [15]. For calculation at room temperature, we subtract a value of 65 meV from the band gap, contributed by the Varshni and polaron shifts, based on the recent work [24]. Besides, we also add the c.m. kinetic energy $K^2/2M$ of 51.8 meV to the relative energy to get the total exciton energy E_{nm}. Regarding the total lifetime, one usually considers both radiative and nonradiative dephasing effects as $1/\tau = 1/\tau_{\mathrm{rad}} + 1/\tau_{\mathrm{nonrad}}$. However, we roughly estimate the exciton lifetime τ by the scaling law $\tau_{\mathrm{rad}} \sim \langle r\rangle^{\xi}$ [28,34] and fit the coefficient from the experiment data for the $1s$ state [30], which suggests the exciton lifetime around 1 ps. The thermal correction to the lifetime based on the formula (8) of about a few percent is not noticeable in Fig. 4.

Figure 4 illustrates the normalized linear optical absorption spectra for the quantum states with principal quantum numbers $n < 4$. This qualitative picture shows the appearance of new peaks when considering the thermal effect. The explanation is based on the deformation of the wave functions, noting that the degeneracy lifting of the excited states and shifts of energies by the magnetic field and the thermoinduced potential also play an important role. Indeed, since the oscillation strength related to these peaks is proportional to the squared modulus of the wave functions at zero electron-hole separation, only the states associated with $|\psi_{nm}(\mathbf{r}=0)|^2 \neq 0$ can be determined by the linear optical absorption spectrum. For the zero-temperature magnetoexciton, only the s-state wave functions have nonvanished oscillation strength while they vanish for all the other states such as p and d; hence, we can only detect the exciton s states from the linear optical response [see Fig. 4 (black and dark blue lines)]. However, because of the thermal effect, the p and d states now become the superposition of other states, including s states. Therefore, we get the signal of the p- and d-state-exciton peaks on the linear optical absorption spectra at room temperature, as shown in Fig. 4 (red line). One can see more details about analytical examination of non-s-state peak emergence in Sec. S-IV D in Supplemental Material [39].

IV. CONCLUSION

By separating the center of mass motion from an exciton in monolayer transition-metal dichalcogenide WSe_2 with a magnetic field, we have pointed out the thermoinduced motional Stark potential on the Schrödinger equation, which was previously neglected. Based on this, we have proposed a mechanism that the thermal motion of the exciton c.m. in a magnetic field could affect the energy spectra of the magnetoexciton. As an observation from our calculation, the thermal-magnetic shifts in the energy spectra are comparable with the polaron shifts caused by the exciton-phonon interaction; thus, they should be considered for magnetoexciton energies at room temperature and can be observed by the shifts of resonance peaks on the absorption spectra. The thermoinduced potential also affects the diamagnetic coefficient and breaks the system's SO(2) symmetry. The symmetry breaking leads to the orbital deformation of the magnetoexciton that indirectly changes the exciton radiative lifetime, which can be observed by examining the width of the resonance peaks on the absorption spectra. Surprisingly, the system's symmetry breaking at room temperature also causes the p-state exciton peaks to emerge on the linear optical absorption spectra, which cannot happen at zero temperature. These results provide another aspect of studying the influence of temperature on magnetoexcitons and could be extended for other monolayer TMDCs such as WS_2. As an outlook, this mechanism could be applied to trions, biexcitons in Dirac materials, and magnetoexcitons originating from the strain-induced pseudomagnetic field.

ACKNOWLEDGMENTS

D.-N. Ly and N.-H.P. are funded by Ho Chi Minh City University of Education Foundation for Science and Technology under Grants No. CS.2019.19.43TD and No. CS.2019.19.44TD. This work is funded by Foundation for Science and Technology of Vietnam Ministry of Education and Training under Grant No. B2022-SPS-09-VL. This work was carried out by the high-performance cluster at Ho Chi Minh City University of Education, Vietnam.

[1] T. C. Berkelbach, M. S. Hybertsen, and D. R. Reichman, Theory of neutral and charged excitons in monolayer transition metal dichalcogenides, Phys. Rev. B **88**, 045318 (2013).

[2] A. Chernikov, T. C. Berkelbach, H. M. Hill, A. Rigosi, Y. Li, B. Aslan, D. R. Reichman, M. S. Hybertsen, and T. F. Heinz, Exciton Binding Energy and Nonhydrogenic Rydberg Series in Monolayer WS_2, Phys. Rev. Lett. **113**, 076802 (2014).

[3] G. Wang, A. Chernikov, M. M. Glazov, T. F. Heinz, X. Marie, T. Amand, and B. Urbaszek, Colloquium: Excitons in atomically thin transition metal dichalcogenides, Rev. Mod. Phys. **90**, 021001 (2018).

[4] M. R. Molas, A. O. Slobodeniuk, K. Nogajewski, M. Bartos, L. Bala, A. Babiński, K. Watanabe, T. Taniguchi, C. Faugeras, and M. Potemski, Energy Spectrum of Two-Dimensional Excitons in a Nonuniform Dielectric Medium, Phys. Rev. Lett. **123**, 136801 (2019).

[5] K. He, N. Kumar, L. Zhao, Z. Wang, K. F. Mak, H. Zhao, and J. Shan, Tightly Bound Excitons in Monolayer WSe_2, Phys. Rev. Lett. **113**, 026803 (2014).

[6] M. M. Ugeda, A. J. Bradley, S.-F. Shi, F. H. da Jornada, Y. Zhang, D. Y. Qiu, W. Ruan, S.-K. Mo, Z. Hussain, Z.-X. Shen, F. Wang, S. G. Louie, and M. F. Crommie, Giant bandgap renormalization and excitonic effects in a monolayer transition metal dichalcogenide semiconductor, Nat. Mater. **13**, 1091 (2014).

[7] Z. Ye, T. Cao, K. O'Brien, H. Zhu, X. Yin, Y. Wang, S. G. Louie, and X. Zhang, Probing excitonic dark states in single-layer tungsten disulphide, Nature (London) **513**, 214 (2014).

[8] H. M. Hill, A. F. Rigosi, C. Roquelet, A. Chernikov, T. C. Berkelbach, D. R. Reichman, M. S. Hybertsen, L. E. Brus, and T. F. Heinz, Observation of excitonic Rydberg states in monolayer MoS_2 and WS_2 by photoluminescence excitation spectroscopy, Nano Lett. **15**, 2992 (2015).

[9] A. Arora, M. Koperski, K. Nogajewski, J. Marcus, C. Faugeras, and M. Potemski, Excitonic resonances in thin films of WSe_2: from monolayer to bulk material, Nanoscale **7**, 10421 (2015).

[10] A. Arora, T. Deilmann, T. Reichenauer, J. Kern, S. Michaelis de Vasconcellos, M. Rohlfing, and R. Bratschitsch, Excited-State Trions in Monolayer WS_2, Phys. Rev. Lett. **123**, 167401 (2019).

[11] A. V. Stier, K. M. McCreary, B. T. Jonker, J. Kono, and S. A. Crooker, Exciton diamagnetic shifts and valley Zeeman effects in monolayer WS_2 and MoS_2 to 65 T, Nat. Commun. **7**, 10643 (2016).

[12] A. V. Stier, N. P. Wilson, G. Clark, X. Xu, and S. A. Crooker, Probing the influence of dielectric environment on excitons in monolayer WSe_2: Insight from high magnetic fields, Nano Lett. **16**, 7054 (2016).

[13] G. Plechinger, P. Nagler, A. Arora, A. Granados del Águila, M. V. Ballottin, T. Frank, P. Steinleitner, M. Gmitra, J. Fabian, P. C. M. Christianen, R. Bratschitsch, C. Schüller, and T. Korn, Excitonic valley effects in monolayer WS_2 under high magnetic fields, Nano Lett. **16**, 7899 (2016).

[14] M. Van der Donck, M. Zarenia, and F. M. Peeters, Excitons, trions, and biexcitons in transition-metal dichalcogenides: Magnetic-field dependence, Phys. Rev. B **97**, 195408 (2018).

[15] A. V. Stier, N. P. Wilson, K. A. Velizhanin, J. Kono, X. Xu, and S. A. Crooker, Magnetooptics of Exciton Rydberg States in a Monolayer Semiconductor, Phys. Rev. Lett. **120**, 057405 (2018).

[16] J. Zipfel, J. Holler, A. A. Mitioglu, M. V. Ballottin, P. Nagler, A. V. Stier, T. Taniguchi, K. Watanabe, S. A. Crooker, P. C. M. Christianen, T. Korn, and A. Chernikov, Spatial extent of the excited exciton states in WS_2 monolayers from diamagnetic shifts, Phys. Rev. B **98**, 075438 (2018).

[17] S.-Y. Chen, Z. Lu, T. Goldstein, J. Tong, A. Chaves, J. Kunstmann, L. S. R. Cavalcante, T. Woźniak, G. Seifert, D. R. Reichman, T. Taniguchi, K. Watanabe, D. Smirnov, and J. Yan, Luminescent emission of excited Rydberg excitons from monolayer WSe_2, Nano Lett. **19**, 2464 (2019).

[18] D.-A. P. Nguyen, D.-N. Ly, D.-N. Le, N.-T. D. Hoang, and V.-H. Le, High-accuracy energy spectra of a two-dimensional exciton screened by reduced dimensionality with the presence of a constant magnetic field, Physica E **113**, 152 (2019).

[19] E. Liu, J. van Baren, T. Taniguchi, K. Watanabe, Y.-C. Chang, and C. H. Lui, Magnetophotoluminescence of exciton Rydberg states in monolayer WSe_2, Phys. Rev. B **99**, 205420 (2019).

[20] M. Goryca, J. Li, A. V. Stier, T. Taniguchi, K. Watanabe, E. Courtade, S. Shree, C. Robert, B. Urbaszek, X. Marie, and S. A. Crooker, Revealing exciton masses and dielectric properties of monolayer semiconductors with high magnetic fields, Nat. Commun. **10**, 4172 (2019).

[21] R. Y. Kezerashvili and A. Spiridonova, Magnetoexcitons in transition metal dichalcogenides monolayers, bilayers, and van der Waals heterostructures, Phys. Rev. Res. **3**, 033078 (2021).

[22] D.-N. Ly, D.-N. Le, D.-A. P. Nguyen, N.-T. D. Hoang, N.-H. Phan, H.-M. L. Nguyen, and V.-H. Le, Retrieval of material properties of monolayer transition-metal dichalcogenides from magnetoexciton energy spectra, arXiv:2303.08089.

[23] F. Lengers, T. Kuhn, and D. E. Reiter, Phonon signatures in spectra of exciton polaritons in transition metal dichalcogenides, Phys. Rev. B **104**, L241301 (2021).

[24] J. C. G. Henriques and N. M. R. Peres, Perturbative approach to the polaron shift of excitons in transition metal dichalcogenides, Phys. Rev. B **103**, L161402 (2021).

[25] Ngoc-Tram D. Hoang, D.-N. Ly, and V.-H. Le, Comment on "Excitons, trions, and biexcitons in transition-metal dichalcogenides: Magnetic-field dependence," Phys. Rev. B **101**, 127401 (2020).

[26] J. E. Avron, I. W. Herbst, and B. Simon, Separation of center of mass in homogeneous magnetic fields, Ann. Phys. (NY) **114**, 431 (1978).

[27] H. Ruder, G. Wunner, H. Herold, and F. Geyer, *Atoms in Strong Magnetic Fields* (Springer-Verlag, Berlin, 1994).

[28] Y. Toyozawa, *Optical Processes in Solids* (Cambridge University, New York, 2003), p. 422.

[29] A. Chernikov, V. Bornwasser, M. Koch, S. Chatterjee, C. N. Böttge, T. Feldtmann, M. Kira, S. W. Koch, T. Wassner, S. Lautenschläger, B. K. Meyer, and M. Eickhoff, Phonon-assisted luminescence of polar semiconductors: Fröhlich coupling versus deformation-potential scattering, Phys. Rev. B **85**, 035201 (2012).

[30] M. Palummo, M. Bernardi, and J. C. Grossman, Exciton radiative lifetimes in two-dimensional transition metal dichalcogenides, Nano Lett. **15**, 2794 (2015).

[31] M. Selig, G. Berghäuser, A. Raja, P. Nagler, C. Schüller, T. F. Heinz, T. Korn, A. Chernikov, E. Malic, and A. Knorr, Excitonic linewidth and coherence lifetime in monolayer transition metal dichalcogenides, Nat. Commun. **7**, 13279 (2016).

[32] D. Van Tuan, M. Yang, and H. Dery, Coulomb interaction in monolayer transition-metal dichalcogenides, Phys. Rev. B **98**, 125308 (2018).

[33] S. Brem, J. Zipfel, M. Selig, A. Raja, L. Waldecker, J. D. Ziegler, T. Taniguchi, K. Watanabe, A. Chernikov, and E. Malic, Intrinsic lifetime of higher excitonic states in tungsten diselenide monolayers, Nanoscale **11**, 12381 (2019).

[34] S. Roux, C. Arnold, F. Paleari, L. Sponza, E. Janzen, J. H. Edgar, B. Toury, C. Journet, V. Garnier, P. Steyer, T. Taniguchi, K. Watanabe, F. Ducastelle, A. Loiseau, and J. Barjon, Radiative lifetime of free excitons in hexagonal boron nitride, Phys. Rev. B **104**, L161203 (2021).

[35] N. S. Rytova, Screened potential of a point charge in a thin film, Mosc. Univ. Phys. Bull. **22**, 30 (1967).

[36] L. V. Keldysh, Coulomb interaction in thin semiconductor and semimetal films, JETP Lett. **29**, 658 (1979).

[37] P. Cudazzo, I. V. Tokatly, and A. Rubio, Dielectric screening in two-dimensional insulators: Implications for excitonic and impurity states in graphene, Phys. Rev. B **84**, 085406 (2011).

[38] E. Hanamura, N. Nagaosa, M. Kumagai, and T. Takagahara, Quantum wells with enhanced exciton effects and optical nonlinearity, Mater. Sci. Eng. B **1**, 255 (1988).

[39] See Supplemental Material at http://link.aps.org/supplemental/10.1103/PhysRevB.107.155410 for detailed derivations of the separation of center-of-mass motion, thermoinduced motional potential, Feranchuk-Komarov operator method for magnetoexciton energies, and analysis of thermoinduced effect by the perturbation method; see also Refs. [55–57] therein.

[40] C. Poellmann, P. Steinleitner, U. Leierseder, P. Nagler, G. Plechinger, M. Porer, R. Bratschitsch, C. Schüller, T. Korn, and R. Huber, Resonant internal quantum transitions and femtosecond radiative decay of excitons in monolayer WSe_2, Nat. Mater. **14**, 889 (2015).

[41] T. Yan, X. Qiao, P. Tan, and X. Zhang, Valley depolarization in monolayer WSe_2, Sci. Rep. **5**, 15625 (2015).

[42] Y. You, X.-X. Zhang, T. C. Berkelbach, M. S. Hybertsen, D. R. Reichman, and T. F. Heinz, Observation of biexcitons in monolayer WSe_2, Nat. Phys. **11**, 477 (2015).

[43] P. Steinleitner, P. Merkl, P. Nagler, J. Mornhinweg, C. Schüller, T. Korn, A. Chernikov, and R. Huber, Direct observation of ultrafast exciton formation in a monolayer of WSe_2, Nano Lett. **17**, 1455 (2017).

[44] D. Farrelly, Motional Stark effect on Rydberg states in crossed electric and magnetic fields, Phys. Lett. A **191**, 265 (1994).

[45] F. Schweiner, P. Rommel, J. Main, and G. Wunner, Exciton-phonon interaction breaking all antiunitary symmetries in external magnetic fields, Phys. Rev. B **96**, 035207 (2017).

[46] K. Tanaka, M. Kobashi, T. Shichiri, T. Yamabe, D. M. Silver, and H. J. Silverstone, LoSurdo-Stark effect for a hydrogenic impurity in a thin layer: Two-dimensional model, Phys. Rev. B **35**, 2513 (1987).

[47] J. C. G. Henriques, H. C. Kamban, T. G. Pedersen, and N. M. R. Peres, Analytical quantitative semiclassical approach to the LoSurdo–Stark effect and ionization in two-dimensional excitons, Phys. Rev. B **102**, 035402 (2020).

[48] H. C. Kamban and T. G. Pedersen, Field-induced dissociation of two-dimensional excitons in transition metal dichalcogenides, Phys. Rev. B **100**, 045307 (2019).

[49] I. Feranchuk, A. Ivanov, V.-H. Le, and A. Ulyanenkov, *Non-Perturbative Description of Quantum Systems* (Springer, New York, 2015).

[50] C. Robert, B. Han, P. Kapuscinski, A. Delhomme, C. Faugeras, T. Amand, M. R. Molas, M. Bartos, K. Watanabe, T. Taniguchi, B. Urbaszek, M. Potemski, and X. Marie, Measurement of the spin-forbidden dark excitons in MoS_2 and $MoSe_2$ monolayers, Nat. Commun. **11**, 4037 (2020).

[51] M. Kira and S. Koch, Many-body correlations and excitonic effects in semiconductor spectroscopy, Prog. Quantum Electron. **30**, 155 (2006).

[52] H. Haug and S. W. Koch, *Quantum Theory of the Optical and Electronic Properties of Semiconductors*, 5th ed. (World Scientific, Singapore, 2009).

[53] S. Wu, L. Cheng, and Q. Wang, Exciton states and absorption spectra in freestanding monolayer transition metal dichalcogenides: A variationally optimized diagonalization method, Phys. Rev. B **100**, 115430 (2019).

[54] S. Wu, Anisotropic exciton states and excitonic absorption spectra in a freestanding monolayer black phosphorus, Physica E **141**, 115238 (2022).

[55] A. P. Prudnikov, Y. A. Brychkov, and O. I. Marichev, *Inverse Laplace Transforms*, Integrals and Series Vol. 5 (Gordon and Breach, New York, 1992).

[56] L. V. Hoang and N. T. Giang, The algebraic method for two-dimensional quantum atomic systems, J. Phys. A: Math. Gen. **26**, 1409 (1993).

[57] Netlib.org. LAPACK: Linear Algebra PACKage, Subroutine dsygvx.f.